Journal of
Ceramic Science
and Technology

J. Ceram. Sci. Technol., **11** [1] 62-72 (2020)
DOI: 10.4416/JCST2019-00076
available online at: http://www.ceramic-science.com

Preparation and Characterization of Reticulated Porous Mullite Coated with Radar-Absorbing Material

S. Lee[1, 3], J.-H. Ha[*1], J. Lee[1], I.-H. Song[1], B. Park[2], S. B. Lee[2], S.-H. Kwon[*3]

[1]Powder and Ceramics Division, Korea Institute of Materials Science, 797 Changwondaero, Seongsan-gu, Changwon, Gyeongsangnam-do, 51508, Republic of Korea
[2]Composites Research Division, Korea Institute of Materials Science, 797 Changwondaero, Seongsan-gu, Changwon, Gyeongsangnam-do, 51508, Republic of Korea
[3]School of Materials Science and Engineering, Pusan National University, 2 Busandaehak-ro 63beon-gil, Geumjeong-gu, Busan, 46241, Republic of Korea

received December 2, 2019; received in revised form February 19, 2020; accepted March 2, 2020

Abstract

Porous ceramics have received much attention because they have excellent thermal and chemical properties. Among the porous ceramics, reticulated porous ceramics (RPCs) have been fabricated for many years. However, as far as the authors know, knowledge of the radar-absorbing properties of RPCs remains insufficient. The authors discussed the feasibility of RPCs, prepared using mullite, as a potential platform that could be coated with a radar-absorbing material (RAM). The results of the experiments in this study were used to determine (1) whether RAM-coated reticulated porous mullite (RPM) could be fabricated with acceptable mechanical strength, and (2) whether RPM could be coated with a RAM while retaining acceptable radar-absorbing properties. Therefore, the structural properties of RPM and the radar-absorption properties of RPM after application of RAM coating were discussed. The compressive strengths of the RPM could be enhanced by controlling the pore densities of commercial polyurethane foams (polymer template) and sintering temperature. The calculated reflection loss (RL) of the 5.74-mm-thick RPM, coated with 10 wt% carbon slurry, approached – 40 dB (99.99 % absorption of radar wave) at 10.0 GHz. The calculated RL of the 17.32-mm-thick RPM, coated with 30 wt% cobalt slurry, approached – 35 dB (99.90 % absorption of the radar wave) at 10.0 GHz.

Keywords: Reticulated porous ceramics, mullite, carbon, cobalt, radar-absorption properties

I. Introduction

Porous ceramics have attracted much research interest [1] for many years because they have many valuable properties, such as low densities [2] and low thermal conductivities [3, 4]. Among the many kinds of porous ceramics, reticulated porous ceramics (RPCs) have inherent 3D-networked structures and high open porosities of 70 – 95 % [5]. Because of these unique properties, RPCs are already actively used in various industrial areas such as filters for molten metal, diesel particulate filters (DPFs), and catalyst supports [5 – 11]. Recently, among RPCs, reticulated porous mullite (RPM) has received scientific interest because of the potential advantages of both RPCs and mullite, which may yield synergetic effects.

Before the radar-absorbing-material (RAM)-coated RPM is addressed, RAMs should be mentioned briefly. Generally, RAMs are purposely designed to absorb incident radar wave from as many incident directions as possible. For decades, RAMs have received special interest because of their radar-absorbing properties (i.e. stealth characteristics), which can be utilized in military applications such as fighter aircraft, and naval ships [12]. However, it is very difficult to fabricate an inexpensive, and lightweight, RAM for coating purposes. RAMs can be fabricated by adding conductive particles to induce dielectric losses by enhancing the conductivity of the platform. Carbon (high conductivity) and cobalt (high Snoek's limit [13]) have been widely used as RAMs for coating because they offer excellent radar-absorbing properties in the X-band (8.2 – 12.4 GHz) [14]. Such RAMs include carbon nanotube-based composites [15, 16], carbon-based composites [17, 18], nickel-cobalt-based composites [19], and cobalt-zinc-based composites [20].

Mullite is among the preferred materials for radar-absorbing applications, particularly because of its high-temperature properties. The advantages of using mullite as a platform for radar-absorbing applications are as follows: (1) Mullite inherently contains glassy phases formed during sintering. Interestingly, above 1 000 °C, the flexural strength and fracture toughness of mullite are increased, because the glassy phases are softened, leading to healing of critical flaws [21]. (2) Mullite has high resistance to creep and a low thermal expansion coefficient (α-alumina = 8×10^{-6} K^{-1}, zirconia = 10×10^{-6} K^{-1}, and mullite = 4.5×10^{-6} K^{-1}) [22], which provide high resistance to thermal shock. (3) The theoretical density of mullite (~ 3.2 g/cm^3)

* Corresponding author: hjhoon@kims.re.kr
co-corresponding author: sehun@pusan.ac.kr

is lower than that of typical ceramics such as alumina (~ 3.96 g/cm^3) and zirconia (~ 5.6 g/cm^3) [22]. (4) The above-mentioned thermomechanical properties are particularly advantageous for the military stealth fighters, which are exposed to severe cyclic rapid heating and cooling during supersonic flight and violent maneuvers. For comparison, the flexural strength and fracture toughness of alumina exhibit steadily decreasing values with increasing temperature, because of its lack of glassy phases [23]. The flexural strength of reticulated porous cordierite also decreases with increasing temperature [24].

Conventional RAM-coated reticulated porous polymers cannot be used at high temperatures or in high load loading conditions because of the inherent drawbacks associated with polymer materials. Therefore, it is worthwhile to investigate RAM-coated RPM as a potential radar-absorbing candidate.

RPM is lightweight and inexpensive. When a RAM is coated on an RPC, the pore characteristics and pore structures of the RPC are important in determining its practical effectiveness. However, there have been very few studies that have investigated reticulated porous alumina (RPA) as a platform for RAM coatings, including the authors' previous studies on carbon-coated [25] and cobalt-coated (unpublished works, Jang-Hoon Ha, *et al.*, 2018) RPA for potential radar-absorbing applications. Moreover, even fewer studies regarding RPM than for RPA have investigated RPM as a versatile platform for RAM coatings. If many studies had already been performed, regarding RAM-coated RPCs, they would not be declassified for long periods because of their military confidentiality.

In this study, the authors tried to utilize RPM as a versatile platform coated with RAMs of carbon and cobalt. However, because of its high open porosity, RPM has low strength and brittleness, which inhibit its further application. Therefore, it is necessary to enhance the mechanical strength of the RAM-coated RPM. The aim of this study is to obtain a RAM-coated RPA that maintains acceptable mechanical strength. Therefore, the authors investigated the effects of mullite slurry compositions and sintering temperatures on the fabrication of an RPM. The effects of the carbon or cobalt slurry compositions on the radar-absorption properties of an RAM-coated RPM material were also investigated. The authors discussed the optimum thickness of the RAM-coated RPM, as well as the optimum RAM content of the coating slurry.

II. Materials and Methods

For the polymer template, commercial polyurethane foams (SKB Tech, Korea) with 400, 1000, and 1800 pores per meter (PPM) and dimensions of 15 cm × 15 cm × 10 mm were used. A mullite slurry was prepared consisting of 260 g mullite (M70, Shibata Yogyo Genryo, Japan), 80 mL distilled water, 1.5 g methyl cellulose, 10 g polyvinyl alcohol (PVA), and 20 mL colloidal silica suspension as an inorganic binder (LUDOX HS-40, Sigma-Aldrich, USA). The mixed mullite slurry was ball-milled for 4 h using alumina balls. Then, the mixed mullite slurry was coated on a polymer template during the coating process; the template was then dried for 24 h at 25 °C. After drying, the coated template was heat-treated at 400 °C for 1 h in air atmosphere to burn off the binder and the polymer template fully, and then sintered at 1 300 – 1 600 °C for 1 h in air atmosphere to sinter the mullite particles. After sintering, the mullite slurry-coated polymer template was converted to RPM.

The RPM was then RAM-coated with carbon. Prior to dip-coating of the carbon onto the RPM, the RPM was coated with 3-aminopropyltrimethoxysilane (APTMS) [26, 27] as a pre-treatment to enhance the adhesion between the RPM and carbon. The carbon slurry consisted of 3 – 10 g carbon as an RAM (Ketjen Black EC-300j, AkzoNobel, Netherlands), 1 g sodium dodecylbenzenesulfonate (SDBS, Sigma-Aldrich, USA) as a dispersant, 100 mL distilled water as a solvent, and 10 g polyvinylpyrrolidone as an organic binder (Sigma-Aldrich, USA). Among the contents in the carbon slurry, Ketjenblack is generally used in various areas because of its high purity [28, 29]. Therefore, Ketjenblack was selected to avoid unexpected side-effects induced by various impurities. The carbon coating slurry was mixed by stirring for 10 min and ultra-sonicating for 10 min. It was then dip-coated on the RPM, and dried fully at room temperature for 24 h.

The RPM was also prepared for cobalt RAM coating. Prior to coating, the specimen was also pre-treated with APTMS [26, 27] as with the carbon coating. The cobalt slurry consisted of 30 – 40 wt% cobalt powder (R125, AOMETAL, Republic of Korea) as an RAM, 54 – 63 wt% of epoxy resin (YD128, Kukdo Chemical, Republic of Korea), and 6 – 7 wt% hardener (KBH1089, Kukdo Chemical, Republic of Korea). The cobalt slurry was coated on the RPM, which was dried fully at room temperature for 24 h.

The compressive strengths of the RPM were measured with an Instron 4206 universal testing machine (Instron, USA) and a full-faced test method. For the measurement of compressive strength, RPM was machined to the dimensions of 20 × 20 × 20 mm. The microstructure of the RAM-coated RPM was investigated with scanning electron microscopy (SEM, JSM-5800, JEOL, Japan). To measure the complex permittivity and permeability of the RAM-coated RPM at 8.2 – 12.4 GHz, an Agilent N5230A analyzer (PNA-L Vector Network Analyzer) was utilized. The radar-wave-absorbing properties were calculated using the scattering parameters of the reflected and transmitted microwaves over 8.2 – 12.4 GHz by employing Agilent 85071E software, which adopted the Nicolson-Ross-Weir method.

III. Results and Discussion

(1) Reticulated porous mullite coated with carbon

Fig. 1 (a) shows the commercial polyurethane foams used as polymer templates (pore densities = 400, 1 000, and 1 800 PPM). Fig. 1 (b) shows the RPMs (pore densities = 400, 1 000, and 1 800 PPM) fabricated with the replica method. The commercial polyurethane foam was immersed in the mullite coating slurry until its strut walls were fully coated with mullite particles in a conventional replica method. The mullite-impregnated polyurethane foam was then squeezed by hand to remove excess mullite slurry, leaving a thin mullite coating layer over the strut walls of the polyurethane foam. At this time, the viscosity of the mullite coating slurry is very important to avoid the occurrences of mullite slurry dripping (insufficient coating) and pore blocking (excessive coating) [1].

Figs. 1 (c) and (d) show a fractured strut wall of as-sintered RPM. This figure illustrates the macroscale voids that are typically generated after the pyrolysis of the polymer template (in this study, the polyurethane foam). RPCs prepared with the replica method with macro voids and large defects generally have poor mechanical properties. These defects are inevitable because the polymer template burn-out process is essential in the replica method. This makes the RPC prone to structural stresses, severely reducing operation life [30]. To alleviate this problem, researchers have attempted to enhance the mechanical properties of RPCs by adopting the pretreatment of the polymer template, multiple slurry coatings, and vacuum infiltration [5, 7, 10]. The authors attempted two methods to enhance the mechanical strength of the RPM. One way is controlling the sintering temperature of the RPM, and the other way is increasing the pore density of the polymer template (polyurethane foam). In a previous study, the multiple slurry coating technique was investigated by the authors. The compressive strength of the RPM itself was significantly enhanced; however, as the number of coatings increased, the thickness of the strut wall was correspondingly increased and the inter-connected pore channels were easily blocked by the viscous mullite coating slurry, which severely inhibited the impregnation of RAM, whether carbon or cobalt. Therefore, only the above-mentioned two approaches may practically achieve the improvement of the compressive strengths of RPM specimens.

In preliminary experiments, the composition of the mullite coating slurry was carefully determined by considering the effects of the weight ratio of the organic binder (PVA) and mullite particles. The dip-coating conditions were also optimized by changing the operating parameters, such as the support withdrawal speed and support dipping time. The densities of the RPM sintered at 1 300 – 1 600 °C are increased proportionally as the pore densities and sintering temperatures increase, as shown in Fig. 2 (a). It can be understood that as the pore density increases, the pore sizes of the RPM decrease, and naturally, the number of the strut walls increases inversely. When the sintering temperature is increased, the sintering reaction is more actively progressed; thus, the degree of densification increases correspondingly.

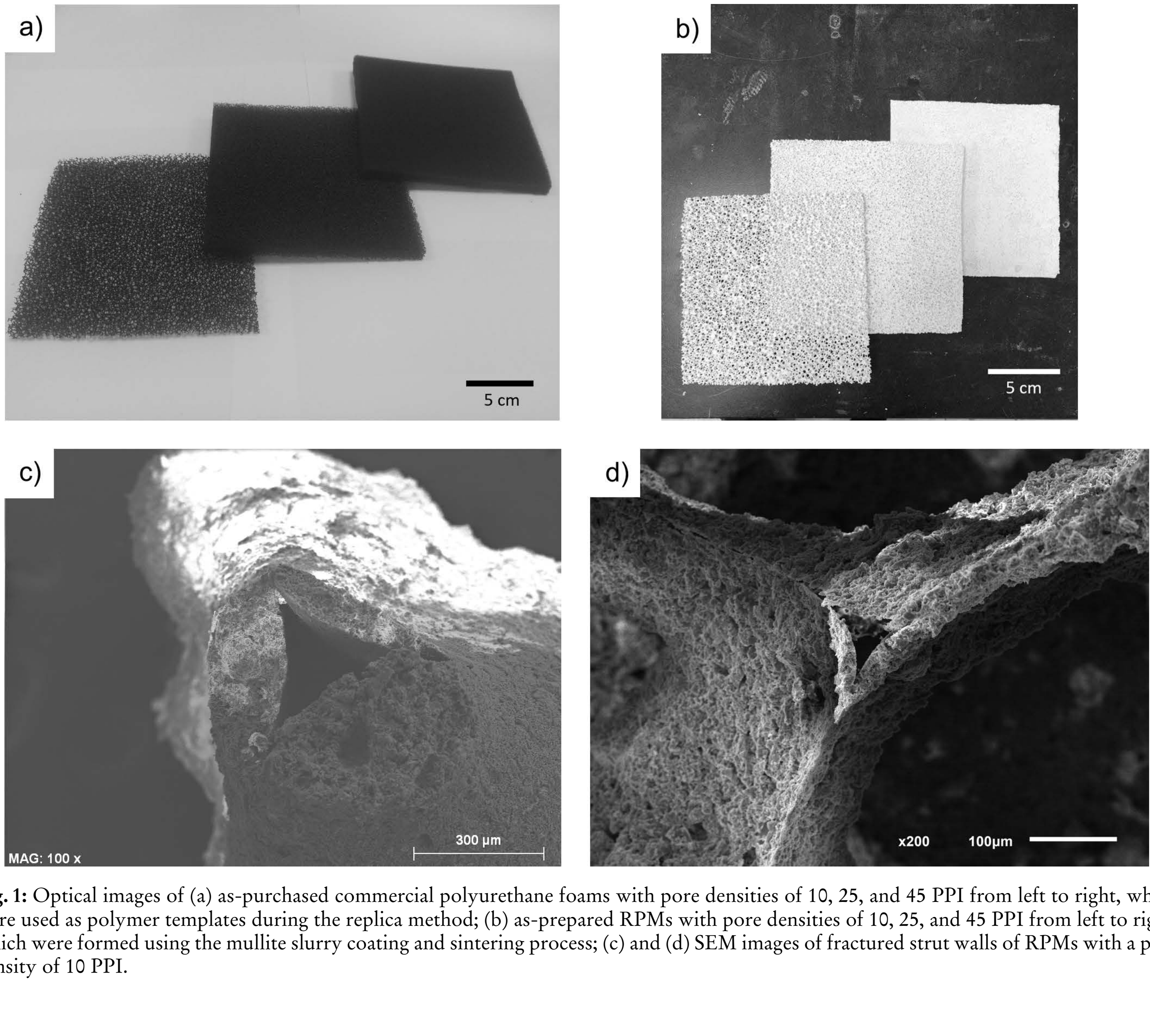

Fig. 1: Optical images of (a) as-purchased commercial polyurethane foams with pore densities of 10, 25, and 45 PPI from left to right, which were used as polymer templates during the replica method; (b) as-prepared RPMs with pore densities of 10, 25, and 45 PPI from left to right, which were formed using the mullite slurry coating and sintering process; (c) and (d) SEM images of fractured strut walls of RPMs with a pore density of 10 PPI.

a)

b)

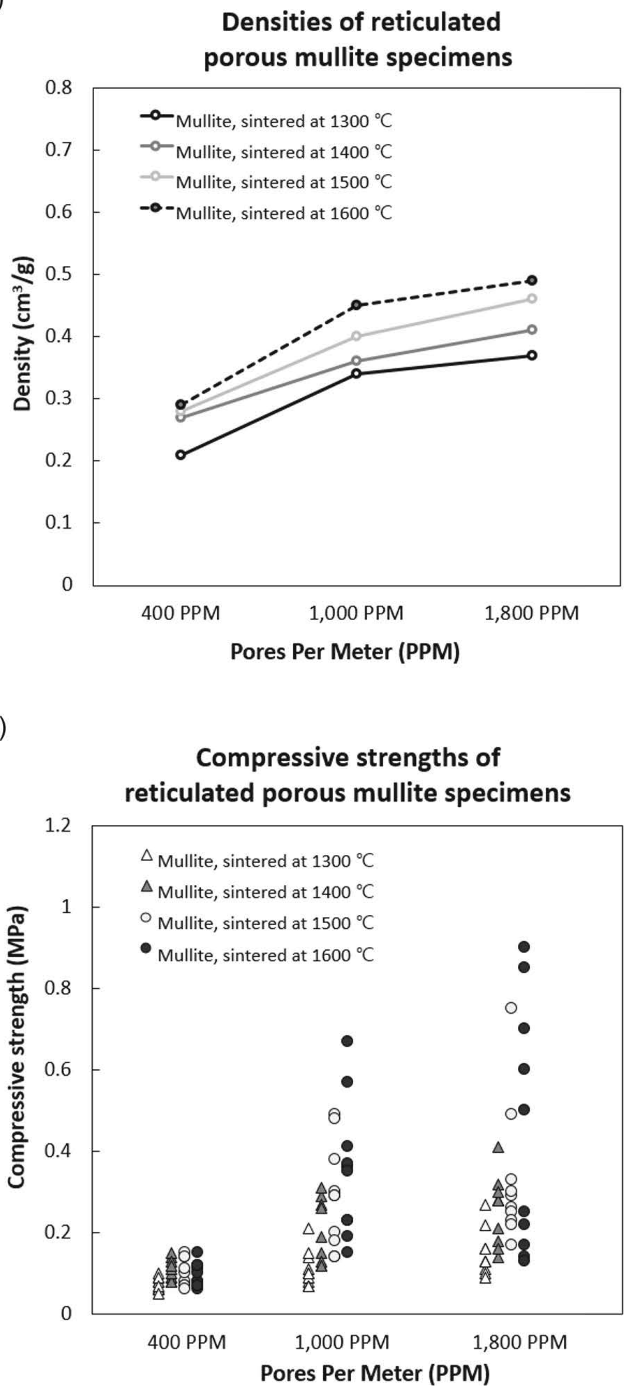

Fig. 2: (a) Densities and (b) compressive strengths of the RPMs sintered at 1 300 – 1600 °C.

The compressive strengths of the RPM sintered at 1 300 – 1 600 °C (pore density = 400, 1 000, and 1 800 PPM) are shown in Fig. 2 (b). The compressive strength of the 400 PPM RPM is not significantly increased when the sintering temperature is increased. It is suggested that the strut walls of the RPM are too sparsely distributed to effectively affect the increase of the overall compressive strength. However, as the pore density of the RPM is increased from 400 PPM to 1 000 PPM, the effect of increasing the sintering temperature on the compressive strength of RPM is increased. The data is scattered because of the inherent brittle fracture behavior of RPC. The authors determined that the compressive strength of the RPM (pore density = 1 800 PPM) was definitely increased as the sintering temperature increased. It may be thought that the compressive strength of the RPM (pore density = 400 PPM) is governed mainly by the sparsely distributed strut walls, not by the sintering temperature. Gradually, the compressive strength of the RPM is affected by the densification of the mullite particles which cover the densely distributed strut walls, as the pore density is increased from 400 PPM to 1 800 PPM. Therefore, the compressive strength of the RPM (pore density = 1 800 PPM) sintered at 1 600 °C had the highest compressive strength. The compressive strengths of the RPM were increased from 0.12 MPa (pore density 400 PPM, sintered at 1 300 °C) to 8.89 MPa (pore density 1 800 PPM, sintered at 1 600 °C) by controlling the sintering temperature and by choosing pore density of the polymer template (polyurethane foams). This trend corresponded well with the previous study on RPA [25].

Fig. 3 shows a typical optical image of the as-prepared RPM (pore density = 400 PPM). Few blocked pores and pore channels of RPM are generated during the mullite slurry coating process. Typical optical images of the RPM coated with 3, 5, and 10 wt% carbon slurries are shown in Fig. 4 (a), (b), and (c), respectively. Few blocked pores and pore channels appear in the RAM-coated RPM.

The electromagnetic properties of RAMs can be expressed by means of the complex permittivity and permeability. The real parts (ε' and μ') of the complex permittivity and permeability represent the storage capabilities of electric and magnetic energy, and the imaginary parts (ε'' and μ'') symbolize the loss of electric and magnetic energy [31]. Note that the real and imaginary parts of complex permeability were assumed as $\mu' = 1$, and $\mu'' = 0$, respectively, because carbon has no magnetic properties, unlike cobalt, which will be discussed below.

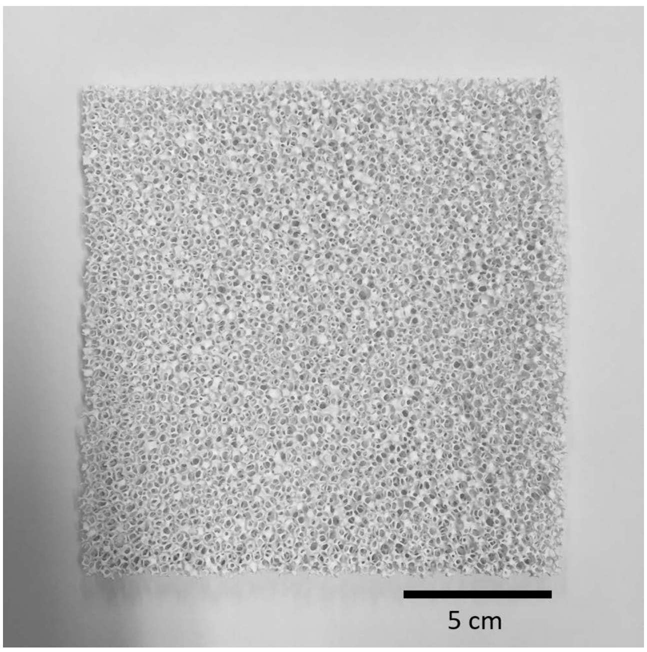

Fig. 3: An optical image of the as-sintered RPM with a pore density of 10 PPI (thickness = 10.50 mm).

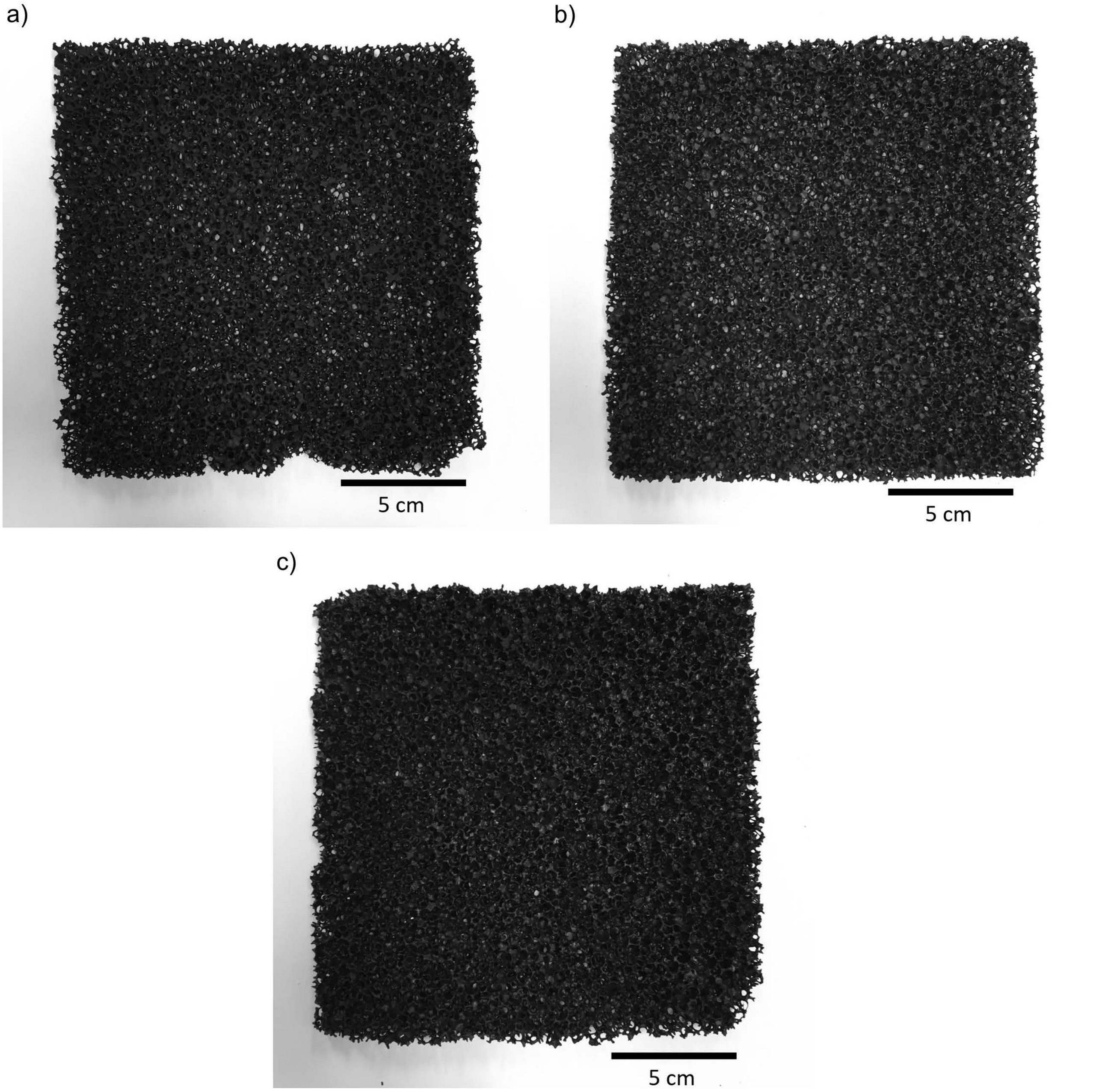

Fig. 4: Typical optical images of the carbon-coated RPMs with a pore density of 10 PPI, which were coated with (a) 3 wt%, (b) 5 wt%, and (c) 10 wt% carbon slurry.

The variation in the real and imaginary parts of the complex permittivity of the as-prepared RPMs, and the RPMs coated with 3, 5, and 10 wt% carbon slurries over the frequency range 8.2 – 12.4 GHz are shown in Fig. 5 (a) and (b). Both the real and imaginary parts of the complex permittivity are increased as the carbon content of the slurry increases. The values of the real part ε' are higher than those of the imaginary part ε'', regardless of the carbon coating on the RPM specimens over the frequency range 8.2 – 12.4 GHz.

These results could be explained based on two important factors. First is the structural factor induced by the porous structure of RPM. The radar-absorbing properties are governed by absorption and the multiple internal reflection of incident electromagnetic radiation in the strut walls of RPM. Hence, the pore structure of RPM causes multiple reflections and scattering of the incident microwaves. Second is the conductive behavior of the carbon particles coated on the RPM matrix. Some of the incident radar waves are absorbed by the carbon particles. The remainder of the incident radar waves propagate through the medium (RPM matrix) at an intensity lower than that of the initial incident radar wave. The pores and pore channels of the RPM enable free movement of the radar waves within the medium, and the RAM present within the medium absorbs some of the radar waves. Note that if the permittivity is too high, the impedance match deteriorates, resulting in strong reflection and weak absorption [32, 33]. Hence, on the basis of the results of preliminary experiments, the authors did not excessively increase the amount of carbon in the coating slurry above 10 wt%. This data corresponds well with studies on carbon-based RAMs by other researchers [34 – 36] and the authors [25].

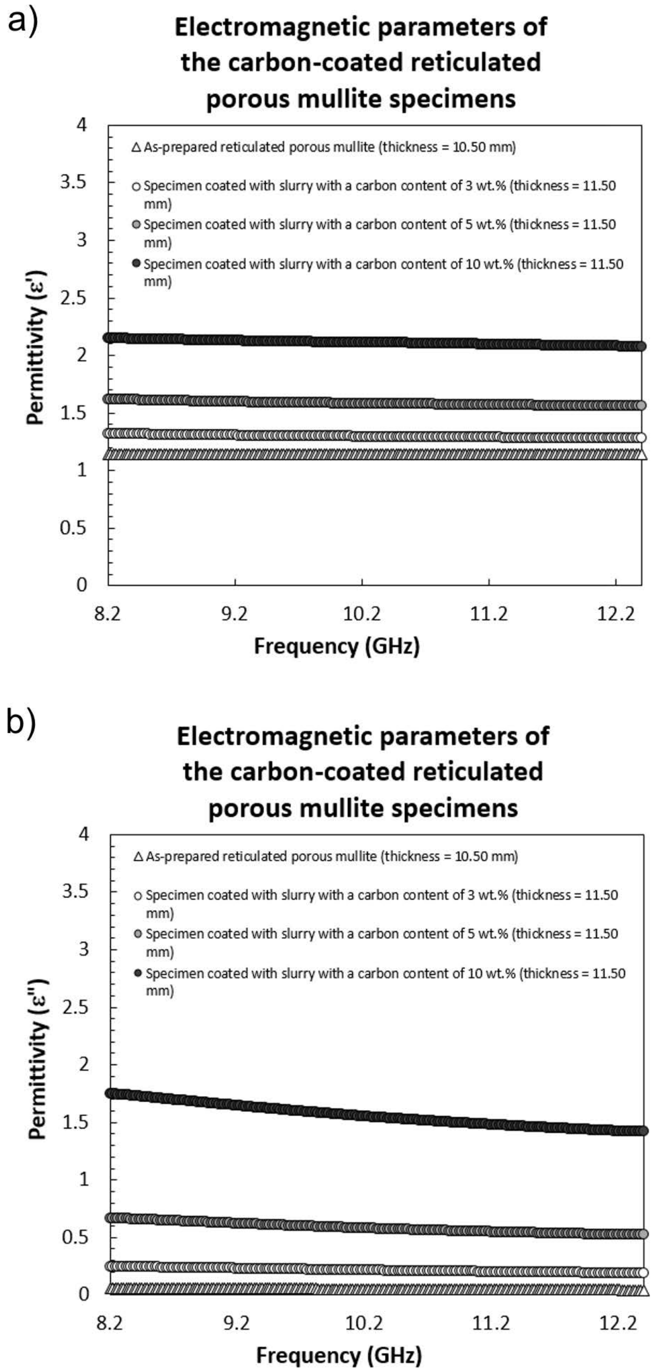

Fig. 5: (a) Real part of complex permittivity, (b) imaginary part of complex permittivity of the RPMs coated with 3, 5, and 10 wt% carbon slurry, and the as-prepared RPM.

The reflection losses (RLs) of the as-prepared RPMs, and the RPMs coated with 3, 5, and 10 wt% carbon slurry were measured over the range 8.2 – 12.4 GHz. The data is plotted in Fig. 6 (a). The RL is derived from the complex permittivity and permeability at a given frequency and radar wave absorber thickness, using the transmission line theory. The measured RL of RPM coated with 10 wt% carbon slurry (thickness = 11.50 mm) is -10 dB at 11.0 GHz, indicating a RL of ≤ -10 dB (90.00 % absorption of the incident radar wave). The RPM coated with 10 wt% carbon slurry has superior absorption properties compared to those of the as-prepared RPM. This is induced by the synergetic combination effect of the RPM matrix and carbon particles, as discussed previously.

Generally, the effective balance between their real and imaginary parts of the permittivity affect the overall radar-absorbing properties of RAM [37]. Carbon, which was used in this study, is a conductive material with large real and imaginary permittivities. If the radar wave is un-matched at a given RAM thickness, the RAM shows weak absorption properties. Therefore, it is very important to control the amount of RAM coated on the RPC, which governs the permittivity and subsequently the radar wave match. Hence, the RPM coated with 10 wt% carbon slurry has better cooperative interaction compared to that of the other RPMs. This may contribute to the superior radar-absorbing properties of the RPM coated with 10 wt% carbon.

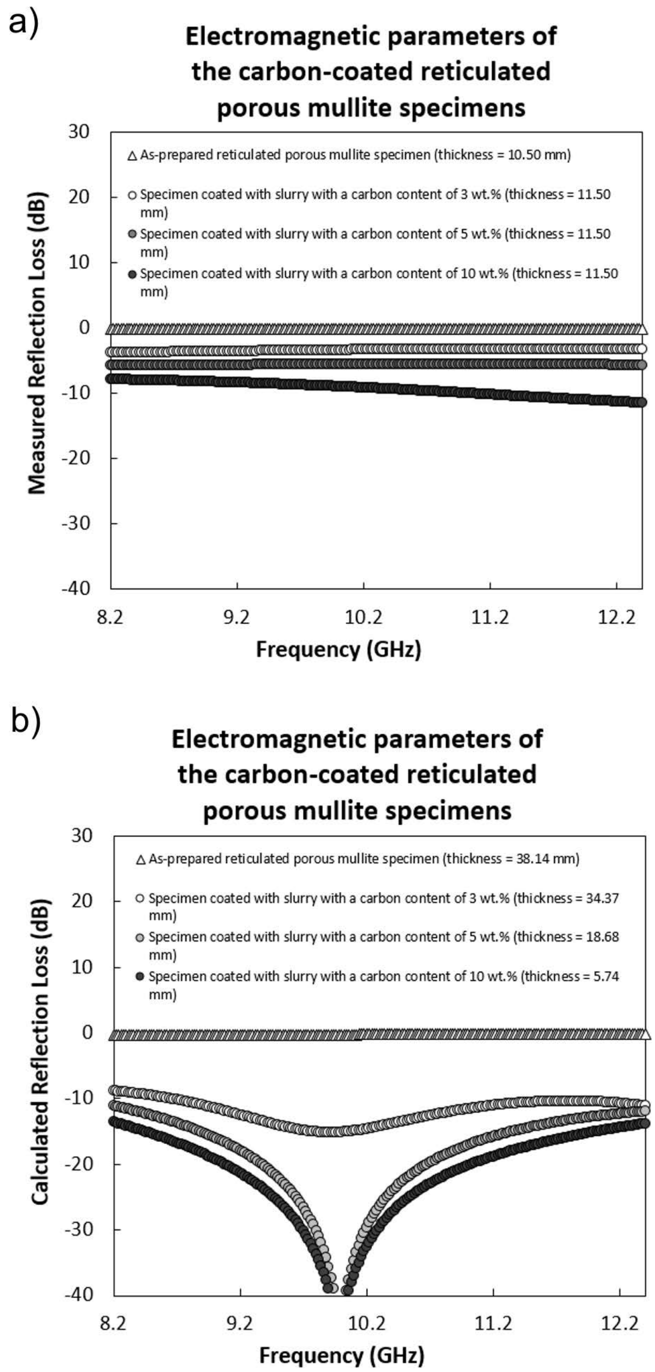

Fig. 6: (a) Measured RL, and (b) calculated RL of the RPMs coated with 3, 5, and 10 wt% carbon slurry, and the as-prepared RPM.

The radar-absorption properties of RAM-coated RPM can be enhanced by changing the RPM thickness, because the characteristic input impedance is a function of thickness. Therefore, when the thickness of a carbon-coated RPM is optimized, the maximum RL can be achieved. However, the calculated optimum RL is possible to determine theoretically, but difficult to achieve experimentally, because the thickness of the RPM is just the replica of the polymer template. The polymer template is usually a commercial polyurethane foam, which offers uniform surface and thickness but is difficult to machine freely. This applies to the PPM value of commercial polyurethane foams for the same reason. Therefore, to obtain the best radar-absorption properties of RAM-coated RPM, the optimized thickness of the carbon-coated RPM was calculated (instead of being fabricated using an actual thickness) using the transmission line theory on the basis of the measured data, as in previous reports [32, 38, 39].

The RL of the as-prepared RPM and those coated with 3, 5, and 10 wt% carbon slurries were calculated over the range 8.2 – 12.4 GHz. The calculated data are plotted in Fig. 6 (b). The calculated RL of the RPMs (thickness = 34.37, 18.68, and 5.74 mm), coated with 3, 5, and 10 wt% carbon slurry, respectively, is -40 dB at 10.0 GHz. This corresponds to 99.99 % absorption of the incident radar wave. In addition, the calculated RL for each of the RPMs coated with 3, 5, and 10 wt% carbon slurries is lower than -10 dB over the frequency range 8.2 – 12.4 GHz. It is observed that as the amount of carbon in the coating slurry increased, the RL remained constant when the thickness of the RPM decreased. It is advantageous that the thickness (directly connected to the weight) of the carbon-coated RPM can be reduced significantly by increasing the amount of carbon in the coating slurry.

These trends are well matched to the previous research on carbon-based RAM, for example, (1) 98.54 % absorption at 11.1 GHz, (thickness = 2.0 mm) [16], (2) 98.4 % absorption at 8 GHz (thickness = 4.0 mm) [15], and (3) 99.5 % absorption at 11.5 GHz (thickness = 4.0 mm) [17].

(2) Reticulated porous mullite coated with cobalt

Typical optical images of the RPMs coated with 30 wt% and 50 wt% cobalt slurries are shown in Figs. 7 (a) and (b). Few blocked pores and pore channels appear during the coating process with slurry with 30 wt% cobalt, as shown in Fig. 7 (a). However, many blocked pores and pore channels appear in the RPM specimen coated with 50 wt% cobalt slurry, as shown in Fig. 7 (b), which inhibits its practical use, although the high cobalt content may significantly promote the radar-absorbing properties.

The variations in real and imaginary parts of complex permittivity of the cobalt-coated RPM specimens over the frequency range 8.2 – 12.4 GHz are shown in Figs. 8 (a) and (b). The values of the real part ε' are higher than those of the imaginary part ε'', regardless of the cobalt coating levels on the RPM specimens. It was obvious that both ε' and ε'' of the cobalt-coated RPM specimens are increased with increasing amounts of cobalt in the coating slurry over the frequency range 8.2 – 12.4 GHz.

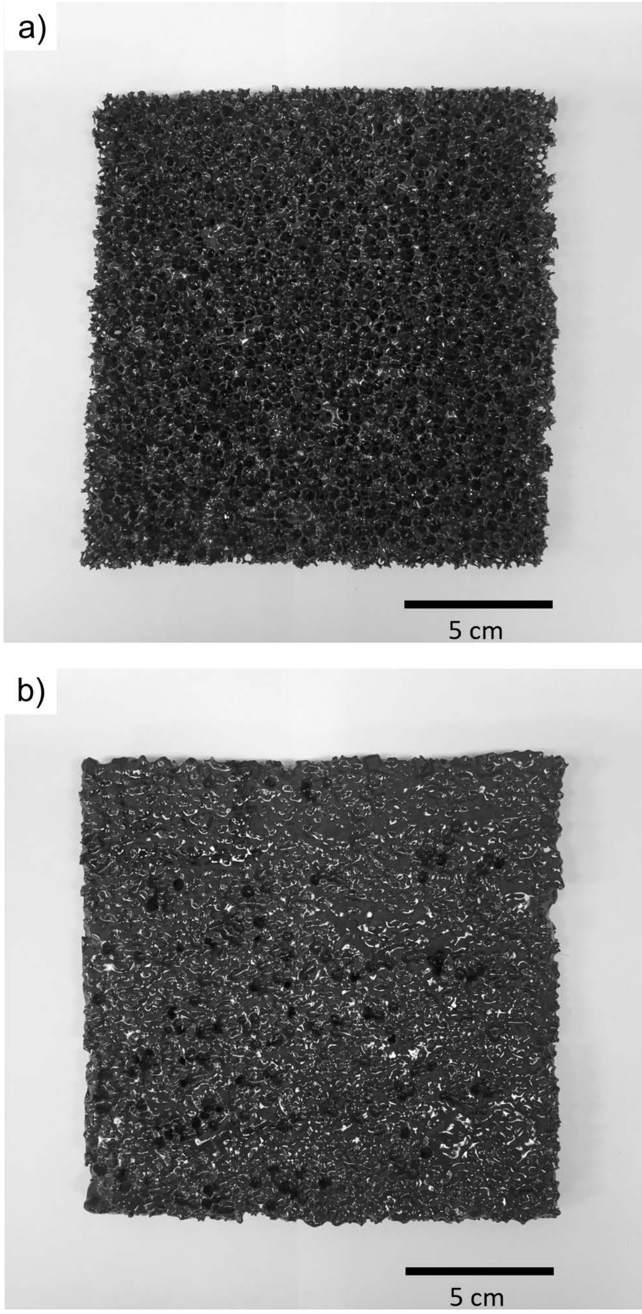

Fig. 7: Typical optical images of the cobalt-coated RPMs with a pore density of 10 PPI, which were coated with (a) 30 wt%, and (b) 50 wt% cobalt slurry.

Figs. 8 (a) and (b) shows the complex permittivities (ε' and ε'') of the as-prepared RPM and the RPMs coated with 30 wt% and 50 wt% cobalt slurries. The complex permittivities (ε' and ε'') are increased as the cobalt content of the slurry increases, related to the conductivity of the cobalt particles incorporated into the porous mullite matrix. The trend seen in the permittivities corresponds well with data previously obtained for RAMs that are nickel-cobalt-based [19] and cobalt-zinc-based [20].

The imaginary part of permeability (μ'') of the RPM coated with 30 wt% cobalt slurry shows a peak at 11.4 GHz, which implies that magnetic resonance occurs. This may cause high-frequency microwave wave absorption, as shown in Fig. 8 (b). As previously discussed with regard to the carbon-coated RPMs, for a specific composite sample, although the electromagnetic parameters (the complex permittivity and permeability) are fixed in the measured frequency range, the peak frequency can still be manipulated by changing the specimen thickness according to the quarter-wavelength condition [40, 41]. This is also significant for the radar-absorbing applications of ferromagnetic metal-based composites such as the cobalt-coated RPM.

The RLs of the as-prepared RPM, and the RPM coated with 30 wt% and 50 wt% cobalt slurry were measured over the range 8.2 – 12.4 GHz. The results are shown in Fig. 9 (a). With RAMs, the RL for a given frequency and absorber thickness is derived from the complex permittivity and permeability and can be modeled with the transmission line-type theory. The authors were disappointed to observe that the measured RL of the cobalt-coated RPM (30 wt% cobalt slurry, thickness = 10.10 mm) is close to 0 dB at frequencies 8.2 – 12.4 GHz, corresponding to a negligible RL. When the amount of cobalt is increased to 50 wt% (12.10 mm thickness), the measured RL of the cobalt-coated RPM is -10 dB at 10.0 GHz, which means 90.00 % absorption of incident radar waves.

Therefore, it is believed that the marginal RLs arose from using a non-resonant thickness of the cobalt-coated RPMs, as with the carbon-coated RPMs.

Again, by choosing an appropriate thickness of cobalt-coated RPM, a maximum RL can be obtained. The RLs of the as-prepared RPM, and the RPM coated with 30 wt% and 50 wt% cobalt slurries were calculated over the range 8.2 – 12.4 GHz. The results are plotted in Fig. 9 (b). The calculated RL of an RPM (thickness 2.90 mm, coated with 50 wt% cobalt) approaches -20 dB at 10.0 GHz (99.00 % absorption of the radar wave). For an RPM with the thickness of 17.32 mm and 30 wt% cobalt-slurry coating, the calculated RL approaches -35 dB at 11.4 GHz (99.90 % absorption of the radar wave).

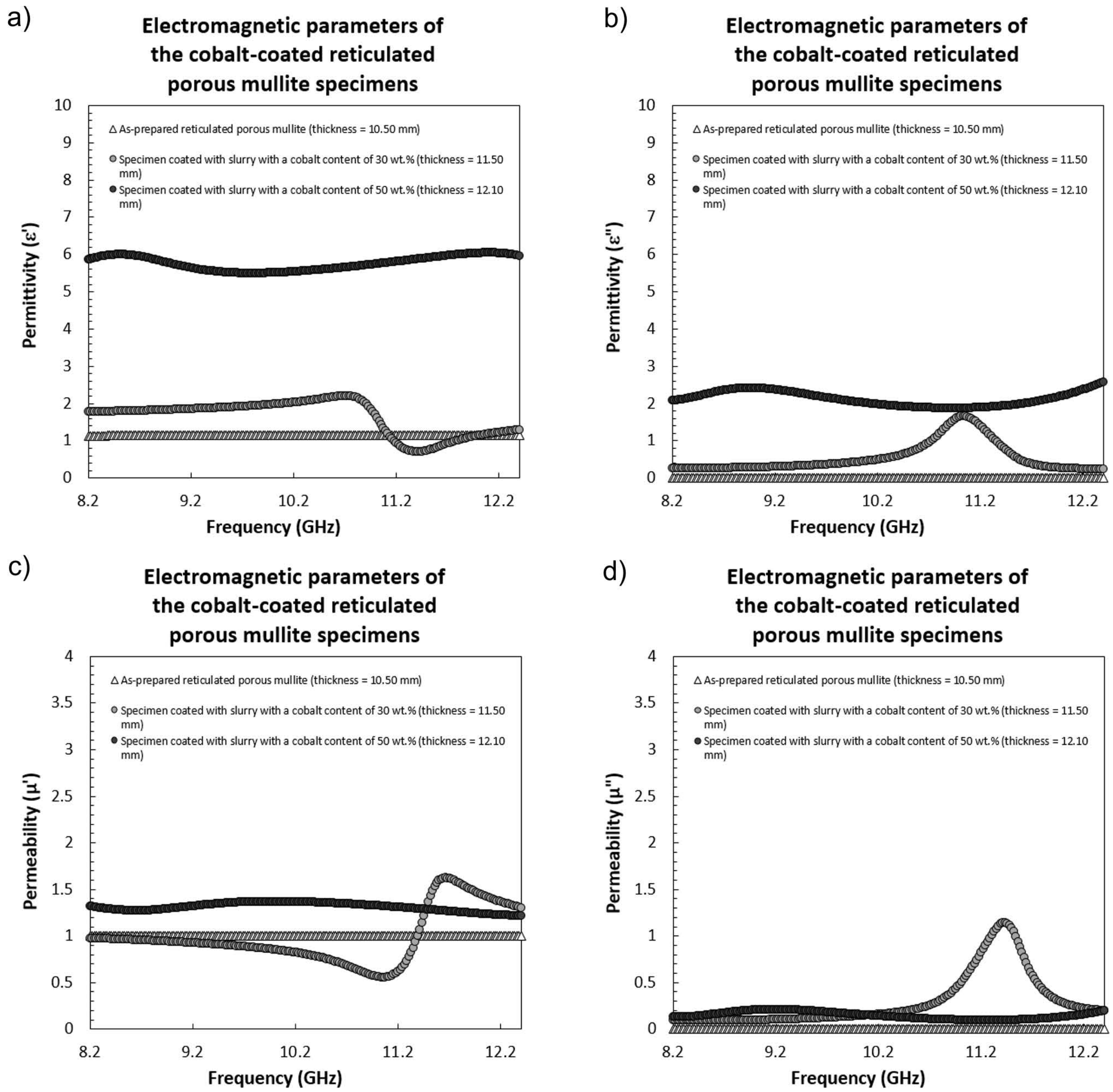

Fig. 8: (a) Real part of complex permittivity, (b) imaginary part of complex permittivity, (c) real part of complex permeability, and (d) imaginary part of complex permeability of the RPMs coated with 30 wt%, and 50 wt% cobalt slurry, and the as-prepared RPM.

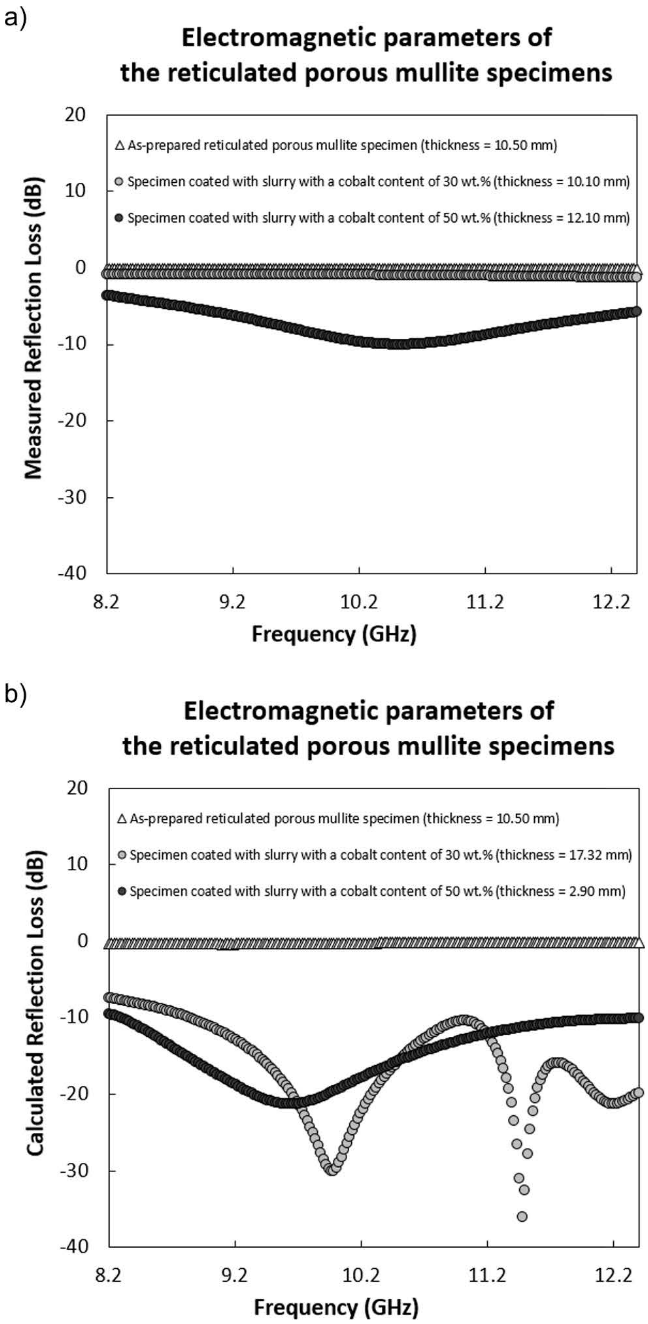

Fig. 9: (a) Measured RL, and (b) calculated RL of the RPMs coated with 30 wt% and 50 wt% cobalt slurry, and the as-prepared RPM.

Over the entire frequency range 8.2 – 12.4 GHz, the calculated RL of RPM coated with 30 or 50 wt% cobalt slurries is at least -10 dB (90.00 % absorption of the radar wave). These calculated values are comparable to the experimental values found in the literature, as previously obtained for RAMs that are nickel-cobalt-based (-33.32 dB, 16.39 GHz, 2.03 mm) [19], and cobalt-zinc-based (-23.6 dB, 7.0 GHz, 4.3 mm) [20].

To compare the calculated RL of carbon or cobalt-coated RPMs with the carbon or cobalt-coated RPAs, the data obtained in this study and in the previous study are plotted together in Fig. 10. The RPM coated with 10 wt% carbon slurry (thickness = 5.74 mm) and the RPA coated with 10 wt% carbon slurry (thickness = 18.40 mm) both exhibit radar-absorbing properties superior to those of the other specimens. These arise from the efficient combination of the porous alumina or mullite matrix and carbon particles for a given thickness. It is difficult to suggest that the radar-absorbing properties of the carbon-coated RPCs are superior to those of cobalt-coated RPCs because of the limited experimental data. It is also difficult to determine (1) whether RPM is superior to RPA as a platform for RAM-coating and (2) which one has superior radar-absorbing properties between RAM-coated RPM and RAM-coated RPA, because of the insufficient experimental data. For example, no high-temperature mechanical strength testing has been performed (one of the advantages of RPM). However, this study demonstrated the feasibility of RAM-coated RPMs as promising candidates for radar-absorption applications, because they are lightweight, show favorable electromagnetic properties, and require inexpensive raw materials. This suggests that various other types of RAM not tried in this study should be further investigated in combination with suitable impregnation methods.

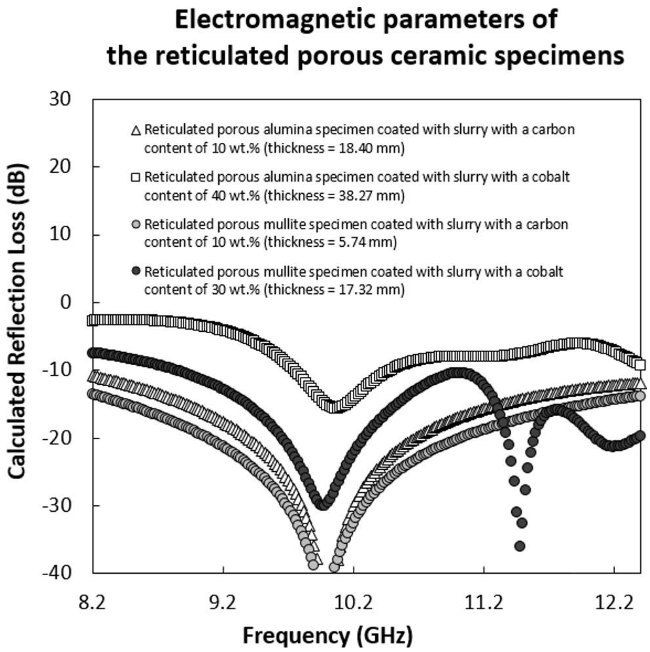

Fig. 10: Calculated RL of the selected RPMs in this study and RPAs in the previous study.

IV. Conclusions

In this study, RPMs were fabricated with a replica method, and subsequently the RAM-coated RPMs were prepared with a dip-coating method. The pore density of the RPM was dependent on the pore density of the commercial polyurethane foam (400, 1 000, and 1 800 PPM). The compressive strengths of the RPMs were increased from 0.08 MPa (400 PPM, sintered at 1 300 °C) to 0.42 MPa (1 800 PPM, sintered at 1 600 °C) by tailoring the sintering temperature and the pore density of the commercial polyurethane foams.

First, the RLs of the carbon-coated RPMs were measured over the range 8.2 – 12.4 GHz. For the RPM coated with 10 wt% carbon slurry (thickness of 11.50 mm), the measured RL was -10 dB overall range (90.00 % absorption of the radar wave). The calculated RL of the RPM coated with

10 wt% carbon slurry (thickness of 5.74 mm) was -40 dB at 10.0 GHz (99.99 % absorption of the radar wave).

Second, the RLs of the cobalt-coated RPMs were also measured over the range 8.2 – 12.4 GHz with the same method used for the above-mentioned carbon-coated RPMs. For the RPM coated with 50 wt% cobalt slurry (thickness of 12.10 mm), the measured RL approached -10 dB at 10.0 GHz (90.00 % absorption of the radar wave). The calculated RL of the RPM coated with 30 wt% cobalt slurry (thickness of 17.32 mm), approached -35 dB at 10.0 GHz (99.90 % absorption of the radar wave).

Third, the calculated RLs of the carbon- or cobalt-coated RPMs and those of the carbon- or cobalt-coated RPAs from the previous study were compared. The RPM coated with 10 wt% carbon slurry (thickness = 5.74 mm) and the RPA coated with 10 wt% carbon slurry (thickness = 18.40 mm) both exhibited radar-absorbing properties superior to those of the other specimens. These valuable findings indicate the feasibility of using RAM-coated RPM for radar-absorption applications.

V. Acknowledgments

This study was supported financially by Fundamental Research Program of the Korean Institute of Materials Science (KIMS), Grant No. PNK6780, and by the Technology Innovation Program (20003782) of the Ministry of Trade, Industry and Energy (Republic of Korea).

References

1 Studart, A.R., Gonzenbach, U.T., Tervoort, E., Gauckler, L.J.: Processing routes to macroporous ceramics: A Review, J. Am. Ceram. Soc., **89**, 1771 – 1789, (2006).

2 Gonzenbach, U.T., Studart, A.R., Steinlin, D., Tervoort, E., Gauckler, L.J.: Processing of particle-stabilized wet foams into porous ceramics, J. Am. Ceram. Soc., **90**, 3407 – 3414, (2007).

3 Santhosh, B., Vakifahmetoglu, C., Ionescu, E., Reitz, A., Albert, B., Soraru, G.D.: Processing and thermal characterization of polymer derived SiCN(O) and SiOC reticulated foams, Ceram. Int., **46**, 5594 – 5601, (2020).

4 Chen, R., Jia, W., Lao, D., Li, S., Hei, D.: Preparation of novel reticulated porous ceramics with hierarchical pore structures, J. Alloy. Compd., **806**, 596 – 602, (2019).

5 Yue, H., Wang, X., Tian, J.: Fabrication of Si_3N4 reticulated porous ceramics reinforced by needle-like β-Si_3N_4, Ceram. Int.,**40**, 8525 – 8532, (2014).

6 Voigt, C., Zienert, T., Schubert, P., Aneziris, C.G., Hubálková, J.: Reticulated porous foam ceramics with different surface chemistries, J. Am. Ceram. Soc., **97**, 2046 – 2053, (2014).

7 Liang, X., Li, Y., Liu, J., Sang, S., Chen, Y., Li, B., Aneziris, C.G.: Improvement of the mechanical properties of SiC reticulated porous ceramics with optimized three-layered struts for porous media combustion, Ceram. Int., **43**, 3741 – 3747, (2017).

8 Voigt, C., Jäckel, E., Aneziris, C.G., Hubálková, J.: Investigations of reticulated porous alumina foam ceramics based on different coating techniques with the aid of μCT and statistical characteristics, Ceram. Int., **39**, 2415 – 2422, (2013).

9 Betke, U., Lieb, A., Scheffler, F., Scheffler, M.: Manufacturing of reticulated open-cellular aluminum nitride ceramic foams from aqueous aln suspensions, Adv. Eng. Mater., **19**, 1600660, (2016).

10 Zhu, X., Jiang, D., Tan, S., Zhang, Z.: Improvement in the strut thickness of reticulated porous ceramics, J. Am. Ceram. Soc., **84**, 1654 – 1656, (2001).

11 Pu, X., Liu, X., Qiu, F., Huang, L.: Novel method to optimize the structure of reticulated porous ceramics, J. Am. Ceram. Soc.,**87**, 1392 – 1394, (2004).

12 Bueno, A.R., Gregori, M.L., Nóbrega, M.C.S.: Microwave-absorbing properties of $Ni_{0.50-x}Zn_{0.50-x}Me_{2x}Fe_2O_4$ (Me=Cu, Mn, Mg) ferrite-wax composite in X-band frequencies, J. Magn. Magn. Mater., **320**, 864 – 870, (2008).

13 Song, N., Gu, S., Wu, Q., Li, C., Zhou, J., Zhang, P., Wang, W., Yue, M.: Facile synthesis and high-frequency performance of $CoFe_2O_4$ nanocubes with different size, J. Magn. Magn. Mater., **451**, 793 – 798, (2018).

14 Choi, I., Lee, D., Lee, D.G.: Radar absorbing composite structures dispersed with nano-conductive particles, Compos. Struct., **122**, 23 – 30, (2015).

15 Munir, A.: Microwave radar absorbing properties of multi-walled carbon nanotubes polymer composites: A Review, Adv. Polym. Technol., **36**, 362 – 370, (2017).

16 Vasconcelos da Silva, L., Pezzin, S.H., Cerqueira Rezende, M., Campos Amico, S.: Glass fiber/carbon nanotubes/epoxy three-component composites as radar absorbing materials, Polym. Compos., **37**, 2277 – 2284, (2016).

17 Pinto, S.S., Rezende, M.C.: Morphological, electromagnetic, and absorbing properties of POMA and PAni/Carbon black composites, J. Electron. Mater., **46**, 4939 – 4947, (2017).

18 Gupta, K.K., Abbas, S.M., Abhyankar, A.C.: Carbon black/polyurethane nanocomposite-coated fabric for microwave attenuation in X & Ku-band (8 – 18 GHz) frequency range, J. Ind. Text., **46**, 510 – 529, (2016).

19 Teber, A., Unver, I., Kavas, H., Aktas, B., Bansal, R.: Knitted radar absorbing materials (RAM) based on nickel-cobalt magnetic materials, J. Magn. Magn. Mater., **406**, 228 – 232, (2016).

20 Poorbafrani, A., Kiani, E.: Enhanced microwave absorption properties in cobalt-zinc ferrite based nanocomposites, J. Magn. Magn. Mater., **416**, 10 – 14, (2016).

21 Osendi, M.I., Baudín, C.: Mechanical properties of mullite materials, J. Eur. Ceram. Soc., **16**, 217 – 224, (1996).

22 Schneider, H., Schreuer, J., Hildmann, B.: Structure and properties of mullite – A review, J. Eur. Ceram. Soc. **28**, 329 – 344, (2008).

23 Munro, R.G.: Evaluated material properties for a sintered alpha-alumina, J. Am. Ceram. Soc., **80**, 1919 – 1928, (1997).

24 Biswas, P., Varaprasad, K., Ramavath, P., Suresh, M.B., Khanra, A.K., Johnson, R.: Development of cordierite based reticulated foams with improved mechanical properties for porous burner applications, Trans. Indian Ceram. Soc., **76**, 56 – 61, (2017).

25 Ha, J.-H., Lee, S., Choi, J.R., Lee, J., Song, I.-H., Lee, S.J., Choi, J.: Development of a carbon-coated reticulated porous alumina material with tailored structural properties for potential radar-absorption applications, Ceram. Int., **43**, 16924 – 16930, (2017).

26 Pasternack, R.M., Rivillon Amy, S., Chabal, Y.J.: Attachment of 3-(Aminopropyl)triethoxysilane on silicon oxide surfaces: dependence on solution temperature, Langmuir, **24**, 12963 – 12971, (2008).

27 Jakša, G., Štefane, B., Kovač, J.: Influence of different solvents on the morphology of APTMS-modified silicon surfaces, Appl. Surf. Sci., **315**, 516 – 522, (2014).

28 Tang, H., Yao, S., Shen, X., Xi, X., Xiao, K.: Lithium-Sulfur batteries with high rate and cycle performance by using multi-layered separators coated with Ketjen Black, Energy Technol-ogy, **5**, 623 – 628, (2017).

29 Wang, D., Shen, Y., Zhang, X., Wu, Z.: Enhanced hydrogen evolution from the MoP/C hybrid by the modification of Ketjen Black, J. Mater. Sci., **52**, 3337 – 3343, (2017).

30 Colombo, P.: Conventional and novel processing methods for cellular ceramics, Philos. T. R. Soc. A, **364**, 109 – 124, (2006).

[31] Zou, T., Wu, Y., Li, H.: Electromagnetic and microwave absorbing properties of carbon-encapsulated cobalt nanoparticles, Mater. Lett., **214**, 280 – 282, (2018).

[32] Meng, X.M., Zhang, X.J., Lu, C., Pan, Y.F., Wang, G.S.: Enhanced absorbing properties of three-phase composites based on a thermoplastic-ceramic matrix ($BaTiO_3$ + PVDF) and carbon black nanoparticles. J. Mater. Chem. A, **2**, 18725 – 18730, (2014).

[33] Smitha, P., Singh, I., Najim, M., Panwar, R., Singh, D., Agarwala, V., Das Varma, G.: Development of thin broad band radar absorbing materials using nanostructured spinel ferrites, J. Mater. Sci.: Mater. Electron., **27**, 7731 – 7737, (2016).

[34] Micheli, D., Apollo, C., Pastore, R., Marchetti, M.: X-Band microwave characterization of carbon-based nanocomposite material, absorption capability comparison and RAS design simulation, Compos. Sci. Technol., **70**, 400 – 409, (2010).

[35] Xi, J., Zhou, E., Liu, Y., Gao, W., Ying, J., Chen, Z., Gao, C.: Wood-based straightway channel structure for high performance microwave absorption, Carbon, **124**, 492 – 498, (2017).

[36] Kolanowska, A., Janas, D., Herman, A.P., Jędrysiak, R.G., GiŻewski, T., Boncel, S.: From blackness to invisibility – Carbon nanotubes role in the attenuation of and shielding from radio waves for stealth technology, Carbon, **126**, 31 – 52, (2018).

[37] Liu, X., Zhang, Z., Wu, Y.: Absorption properties of carbon black/silicon carbide microwave absorbers, Compo. Part B: Eng., **42**, 326 – 329, (2011).

[38] Du, Y., Liu, W., Qiang, R., Wang, Y., Han, X., Ma, J., Xu, P.: Shell thickness-dependent microwave absorption of core-shell Fe_3O_4@C composites, ACS Appl. Mater. Inter., **6**, 12997 – 13006, (2014).

[39] Kong, L., Yin, X., Zhang, Y., Yuan, X., Li, Q., Ye, F., Cheng, L., Zhang, L.: Electromagnetic wave absorption properties of reduced graphene oxide modified by maghemite colloidal nanoparticle clusters, J. Phys. Chem. C **117**, 19701 – 19711, (2013).

[40] Kong, I., Hj Ahmad, S., Hj Abdullah, M., Hui, D., Nazlim Yusoff, A., Puryanti, D.: Magnetic and microwave absorbing properties of magnetite-thermoplastic natural rubber nanocomposites, J. Magn. Magn. Mater., **322**, 3401 – 3409, (2010).

[41] Wang, B., Wei, J., Yang, Y., Wang, T., Li, F.: Investigation on peak frequency of the microwave absorption for carbonyl iron/epoxy resin composite, J. Magn. Magn. Mater., **323**, 1101 – 1103, (2011).